 CMES, vol.89, no.4, pp.263-281, 2012

Sound Power Radiation Sensitivity and Variability Using a 'Hybrid' Numerical Model

Max de Castro Magalhaes[1]

Abstract: The main objective is to develop a 'hybrid' numerical method for predicting sound power radiated from honey-comb panels and analyze the sensitivity and variability of it to different boundary conditions. The honey-comb panels are mainly used on the aerospace, mechanical and civil engineering design. The method used herein is a combination of the Finite Element Method and the Jinc Function Approach. The original contribution of this paper is therefore to show the sensitivity of sound power radiated from a honey-comb panel using a 'hybrid' method which is simple and efficient on tackling sound radiation problems for complex orthotropic panels, especially during the design process. It is believed that this is the first time honey-comb panels have been investigated in terms of sound radiation efficiency using this method. Some background information about the 'hybrid' method is provided as a basis for assisting the understanding of the process. The results obtained using 'typical' boundary conditions, i.e. simply-supported, clamped and free boundaries, are compared to those obtained using more complex boundary conditions which are based on pinned points randomly located along the panel boundary. Finally, conclusions are drawn based on the analysis of the results and the extension to alternative acoustic systems.

Keywords: 'Hybrid' method; FE simulations; honey-comb material; sound radiation

Nomenclature

D	bending rigidity
F	arbitrary complex force in the x, y position on the panel
L_x, L_y	panel dimensions in the x, y directions
S	area of the flexible partition
a	generalized coordinates of the component displacements

[1] Corresponding author, E-mail: maxdcm@gmail.com. Department of Structural Engineering, Federal University of Minas Gerais, Belo Horizonte 31270901, Brazil

c_O	sound speed in air
h	thickness of the flexible partition
k_a	acoustic wavenumber
k_s	structural trace wavenumber of the panel
m,n	subscript for normal modes
t	time.
$u(x,y)$	normal displacement function at position (x,y)
x,y	cartesian coordinate system used for the plate
$\bar{\varepsilon}$	generalized coordinates of the component displacements
η	plate damping loss factor
ρ_o	density of air
ρ	density of the flexible partition
φ_{nm}	matrix of normal displacement modes
ω	angular frequency (rad/s)
ω_{mn}	natural frequency of the plate

1 Introduction

The use of honey-comb material are popular are popular among mechanical, civil and aerospatial engineers and acoustic space designers (e.g. home cinemas, computer audio, public address systems, etc.). They are important not only for their slender dimensions but also for their high stiffness, lightweight and non-combustibility properties. However they provide very little sound absorption in a broadband range [Pan, Guo and Ayres (2005)].

Results on acoustic treatment technology of honeycomb material to improve noise transmission loss characteristics of light-weight panels were presented by Huang Wen-chao and Ng Chung-fai (1998). A prediction model was shown to describe the transmission loss of the honeycomb panels based on the knowledge of their structural modal parameters. A series of test specimens with aluminum sheets, and fiber reinforced concrete sheets as added on panels, were used to investigate the effect of stiffness and damping on noise transmission loss of the honeycomb sandwich panels. Comparison of the experimental results showed that the techniques using acoustic treatment of added-on honeycomb stiffened structure and damping material to reduce the noise transmission were effective. Some practical honeycomb panels design approach was then developed for achieving transmission loss greater than mass law in the frequency band of interest.

Another important paper [Bouayed and Hamdi (2012)] presented numerical and experimental validation of results obtained by a shell finite element, which was developed for modeling of the dynamic behavior of sandwich multilayered structures

with a viscoelastic core. The proposed shell finite element was very easy to implement in existing finite element solvers, since it uses only the displacements as degrees of freedom at external faces and at inter-layer interfaces. The displacement field was linearly interpolated in the thickness direction of each layer, and analytical integration was made in the thickness direction in order to avoid meshing of each sandwich layer by solid elements. Only the two dimensional mid-surface of reference was meshed, facilitating the mesh generation task.

Recently, various researchers have concentrated their work on presenting the main advantages of planar honey-comb panels in terms of its mechanical properties in comparison to the traditional ones. However, the physical understanding of their performance in terms of sound radiation has not been fully understood yet. Usually, different honey-comb panels have different dynamic properties in terms of stiffness and weight. Most manufacturers have tried to control the dynamic parameters which can produce perceptual differences on structural design.

Thus, it is fundamental to determine which relevant dynamic criteria should be used in order to characterize the panel structural utility. In addition, the perception of sound radiated from honey-comb panels is greatly influenced by the surrounded fluid in which it is immersed. The main question that remains unanswered is: what are the characteristics of honey-comb panels as sound radiators which in turn lead to damping radiation? The aim of this paper is to try to answer at least part of this question using a 'hybrid' method to investigate the variability of sound radiated from honey-comb panels to different boundary conditions. As an example, this alternative hybrid-model was considered herein for the prediction of the sound radiated from a baffled panel supported on five-pinned points located along its boundary randomly.

The effects of panel boundaries on sound radiation, including a comparison with an infinite panel have been discussed by several researchers [Pierce (1981); Fahy (1985); Leppington (1982)]. A simple two-dimensional model has been used for evaluating the sound radiation characteristics of finite panels. The analysis of the radiation, through a baffled plate of finite width and infinite length, was conducted rigorously. The effects of panel size were verified in regions below, above and at the critical frequency. Estimates of averaged response over a particular frequency range have also been presented. The literature survey has revealed that a significant amount of work has concentrated on analyzing sound radiation of simply-supported panels.

The hybrid model considered uses a combination of results obtained via numerical simulations and Jinc functions [Langley (2007)]. The Finite Element Method (FEM) was used as the numerical framework for alternative model. As well known, FE models do not have the restriction of simple system geometries, but for com-

putational and accuracy reasons are applicable primarily to low frequency predictions. Basically, the structural modes were obtained from FE models and then applied to the Jinc-function methodology. The Jinc function approach for the prediction of sound radiated from panels was initially developed and applied to simply-supported panels located in a baffle. Most sound radiation problems require a three-dimensional model for better representation of the sound field distribution. The application of Jinc function description is only appropriate at frequency bands lower than the one that corresponds to propagating bending waves that have a half wavelength larger than the grid spacing of the mesh [Langley (2007)]. The Jinc function approach considers an analytical description of the sound radiation at the panel interface and only requires the normal *in-vacuo* structural modes with the relevant boundary conditions. It allows the geometric parameters of the system to be incorporated into the models and subsequent predictions. Subsequently, the frequency response of the system is obtained.

Radiated sound power on the shell wall along the axial direction and the influence of different parameters on the results are studied in ref. [Yan, J.; Li, T.Y.; Liu, J.X.; Zhu, X. (2006)]. A conclusion was drawn that the stiffeners have a great influence at low and high frequencies while have a slight influence at intermediate frequencies for low circumferential mode orders. The results gave some guidelines for noise reduction of this kind of shell.

Recently work has compared sensing the number of vibration modes to the number of orthogonal contributors to radiated power [Hill, S.G.; Tanaka, N.; Iwamoto, H. (2009)]. The required number of vibration modes was based on the proximity of the structural mode resonance frequency and the excitation frequency. This technique resulted in a valid estimate of radiated power, it was shown that the number of structural modes could be minimized by first considering orthogonal radiators based on structural mode amplitudes. Two disturbance cases were considered: a point force and an even disturbance coupling to each structural mode. Also, under these conditions the practicality of estimating the number of orthogonal radiators when it is assumed that each contributor is equal in amplitude was examined. Finally in an attempt to optimism the number of signals to be sensed, a variable error margin for the estimate of power, based on the ratio of the sound power at each frequency to the maximum peak in the considered frequency range was proposed and analyzed.

An improved SEA model for predicting more accurate structural response and noise reduction of acoustical enclosures was presented by [Y. Lei; J. Pan; M.P. Sheng (2011)]. The modeling technique proposed by Renji et al. (2001), that the non-resonant response of every flexible panel is treated as a structural subsystem, was referred in SEA modeling. More accurate transmission coefficient of finite panels

presented by Davy, J.L (is also adopted in the improved model. In the aim of verifying the prediction, experiment was completed. To ensure the reliability of the measured results, both the sound pressure method and the sound intensity method were applied to measure the radiated power from the enclosure.

An article by Cherrier, O.; Pommier-Budinger, V.; Simon, F. (2012) focused on acoustic resonators made of perforated sheets bonded onto honeycomb cavities. This kind of resonators can used in adverse conditions such as high temperature, dirt and mechanical constraints. For all these reasons, they are widely used in aeronautic applications. The acoustic properties were directly linked to the size, shape and porosity of holes and to the thickness of air gaps.

In summary, the main objective of this study is the development and implementation of a new 'hybrid' method which is a 'mixing' of two well-known methods namely: the Finite Element Method and the Jinc function method. In addition, it is also investigated the influence of the boundary conditions on the total sound power radiated. Some results are compared to those obtained using classical boundary conditions, such as the simply-supported, clamped and free boundary cases. Conclusions on the use of this alternative method and its subsequent application to structural radiation problems are briefly presented.

2 Method – Procedure

2.1 Overview of the procedure

The flat honey-comb panel used herein was a flat rectangular plate assumed to be isotropic and homogeneous. It was composed of a honeycomb core layer between two plastic face-sheets (see Fig. 1).

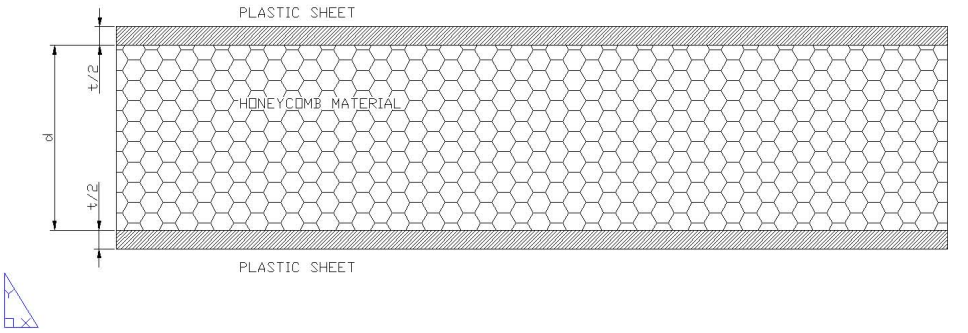

Figure 1: A honey-comb type panel composed of two different materials: plastic layers and a honeycomb core with thickness equal to t/2= 0.1mm and d =5mm respectively

The analyses were performed on four distinct stages as follow: First, experimental tests were carried out in order to obtain the elastic constants and damping of the panel material [8]. Second, a FE model was used in order to obtain the mode shapes (and their corresponding natural frequencies) for a simply-supported plate (flat panel), and consequently to validate the FE model against its analytical counterpart. Third, FE simulations were performed for more complex boundary conditions and the corresponding sets of normal modes $\phi_p(z,y)$ extracted and stored. Finally, a fluid-structure model was developed and implemented in MATLAB for the evaluation of the average sound power radiated.

2.2 Material properties of honey-comb panels

The panel sample considered on the experimental tests had density equal to 131.47 Kg/m^3. Its dimension was 210mm x 297mm x 5mm. For the elastic properties, the procedure adopted was based on measurements of the resonant frequencies of low-frequency modes of thin rectangular plates with free edges. The method of Chladni patterns was used for the measurement of the mode frequencies, as it is a cheap method compared to the one which uses laser vibrometer. Some of the first few vibration modes of a free-edged rectangular honey-comb panel are shown in Figs. 2 and 3.Thus, the four elastic constants D_1, D_2,D_3 and D_4 were deduced from the frequency measurements f_5, ($f_{X,R}$), f_2 and f_1 respectively [McIntyre and Woodhouse (1988)].

Although the ring mode is not shown herein, its corresponding frequency f_R was

(a) (b)

Figure 2: Some of the first few vibration modes of a free-edged rectangular honey-comb samples using the Chladni method; a) Mode 1 is approximately pure twisting motion (f_1=107 Hz); b) Mode 2 is one-dimensional bending-beam mode in the plate-width direction (f_2=238 Hz)

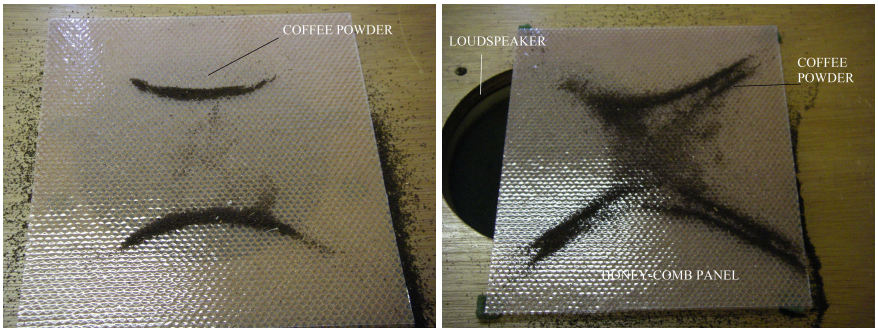

(a) (b)

Figure 3: a) Mode 5 is one-dimensional bending-beam mode in the plate-length direction (f_5=147 Hz); b) X-mode, (f_x = 221 Hz)

equal to 272 Hz. The elastic properties measured are: D_1=76 MPa; D_2=32 MPa; D_3=46 MPa; D_4=71 MPa. The equivalent Young's modulus are: E_x=845 MPa and E_y=845 MPa. In addition, the Poisson ratio measured was 0.24.

For the damping measurement, the modal damping factor was deduced from the measured transfer function applying the half-power bandwidth method. The averaged value obtained for the quality factor was 50. Thus, the loss factor of the material was 0.02. Alternatively, the loss factor was also measured using the laser vibrometer on the mounted panel. It was equal to 0.05. It is believed that a higher value for the loss factor was found due to the damping effect of the boundary. It is seen that the honey-comb panel tested comprises 4 driving points and 5 clamps (see Fig. 4 below).

3 Numerical simulations using the 'hybrid' method

In this section, numerical simulations are presented for different boundary conditions that may be considered, for instance, on the design process of any structural panels. The flat panel normal modes were found numerically in advance of applying the Jinc function approach. The frequency range 0-1200 Hz was considered on the predictions. The analyses were performed on three distinct stages as follows. Firstly, a particular commercial FE software was used in order to obtain the mode shapes (and their corresponding natural frequencies) for the simply-supported case, and consequently to validate the FE model against its analytical counterpart. Secondly, FE simulations were performed for different boundary conditions and the corresponding mode shapes extracted and stored. Finally, the sound power radiated by a honey-comb panel was calculated for each case, using the Jinc function

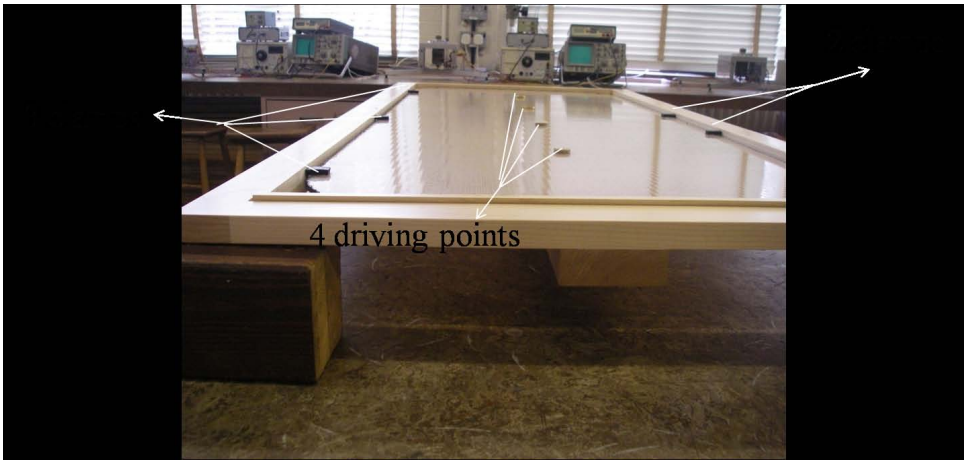

Figure 4: Mounted honey-comb panel used for the experimental tests. It comprises 4 driving points along its middle horizontal plane and 5 clamps (simply-supported points) along its perimeter.

approach.

As mentioned before, a flexible panel made of honey-comb material was considered on the numerical simulations. It had dimensions equal to 485mm x 1220mm x 5mm. The panel critical frequency was f_c = 4991 Hz. The modal density and modal overlap factor were 0.08 modes/Hz and 1.91 @ 1.2 kHz respectively. In all cases four coherent point loads were applied on the centre line of the panel in order to simulate the real case (see Fig. 4).

3.1 The validation of the FE model for the simply-supported case

The first numerical example to be considered was a simply-supported panel, as it seems sensible to begin with the simplest mode shapes. A simply-supported flat plate has mode shapes and frequencies given by [Fahy (1985); Cremer (2005)]

$$\varphi_{mn}(x,y) = \frac{2}{\sqrt{\rho\, h L_x L_y}} \sin\left(\frac{n\pi x}{L_x}\right) \sin\left(\frac{n\pi y}{L_y}\right) \tag{1}$$

$$\omega_{nm}^2 = \left(\frac{D}{\rho\, h}\right)\left[\left(\frac{n\pi}{L_x}\right) + \left(\frac{m\pi}{L_y}\right)\right]^2 \tag{2}$$

where L_x, L_y are the plate dimensions, h is the thickness, ρ is the density of the plate material and D is the bending rigidity. The response (normal displacement

to the plate surface) of the plate to a harmonic point force excitation at position (x_o, y_o) and at frequency ω is given by [Fahy (1985); Cremer (2005)]

$$u(x,y,\omega) = \sum_n \sum_m \left[\frac{F\,\varphi_{nm}(x,y)\,\varphi_{nm}(x_o,y_o)}{\omega_{nm}^2(1+i\eta) - \omega^2} \right] \tag{3}$$

where η is the plate damping loss factor and F is the point force excitation. Alternatively, the response of the plate $u(x,y,\omega)$ may be predicted considering the fluid-structure interaction as described in reference [Magalhaes and Ferguson (2005)]. Fig. 5 shows a comparison between the total energy of a simply-supported plate using a FE model and the analytical model. The plate velocity for the analytical model was obtained using first order derivative of Equation (3).

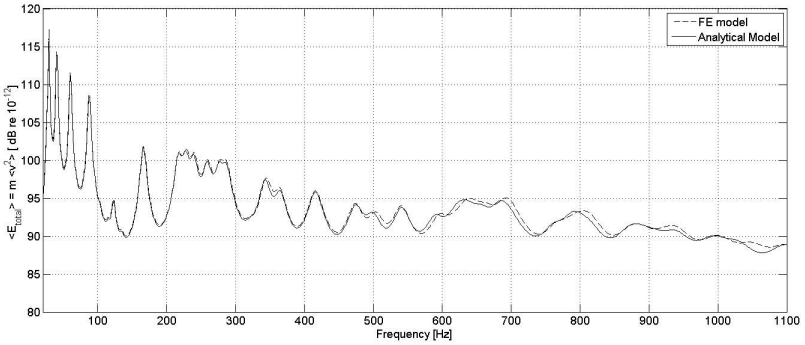

Figure 5: Comparison between the sound energy obtained via FE and analytical models

3.2 Definition of the sets of normal modes via the FE model

The model was designed to be general enough to allow different edge conditions to be imposed. Figs. 6 and 7 show the FE mesh and the corresponding vibration configurations for modes 1, 2, 3, 4, 50 and 185. The Finite Element mesh used on the simulations was composed of 4,492 shell-type elements and 4,636 nodes.

3.3 Prediction of the sound power radiated using the 'Jinc' approach

The time-average space-average sound power radiated P_{rad} by a plate inserted in an infinite baffle can be computed efficiently using the Jinc function approach. Although this method is not as general as BEM or FEM, it allows much faster analysis of the acoustical power radiated from simple planar structures. The surface

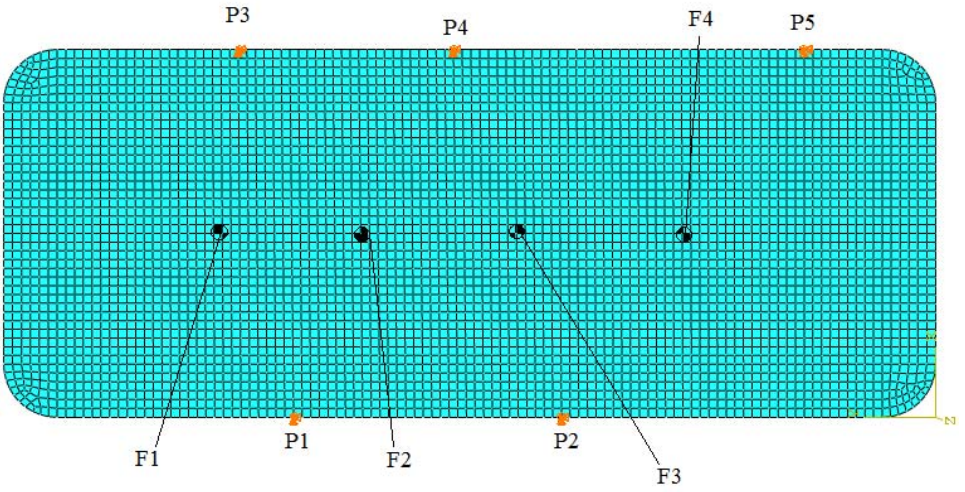

Figure 6: Finite Element mesh used on the simulations (4,492 shell-type elements and 4,636 nodes). The panel boundary is supported by five-simply-supported points. Four harmonic forces are applied to the panel.

displacement of the structure is described by using a grid of *Jinc* function wavelets (see Fig. 8). A *Jinc* function is as

$$Jinc = \frac{J_1(x)}{x} \tag{4}$$

where $J_1(x)$ is the Bessel function. The jinc function allows for a quick calculation of acoustic power.

The radiated acoustic power can be obtained from the dynamic stiffness of the structure via symmetric wavelets. Thus, the power radiated is then given by

$$P_{rad} = \left(\frac{\omega}{2}\right) \mathbf{a}^{*T} Im\{\mathbf{D}\}\, \mathbf{a} \tag{5}$$

where $\mathbf{D}$ is the acoustic dynamic stiffness matrix expressed in Jin function coordinates and $\mathbf{a}$ is the amplitude of the jinc function centred at grid point location $\mathbf{x}_n$. It has been shown in reference [Langley (2007)] that

$$Im\{D_{ij}\} = \frac{8\,\pi\,\omega\,\rho_o c_o k_a^2}{k_s^4}\,\mathrm{sinc}(k_a\, r_{ij}), \quad \mathbf{a} = \frac{\pi}{2} u(\mathbf{x}_n), \tag{6}$$

where $r_{ij} = \left|x_i - x_j\right|$, $k_s = \sqrt{2}\,\frac{\pi}{\delta}$, $u(\mathbf{x}_n)$ is the complex amplitude of the panel normal displacement, ω is the angular frequency (rad/s), ρ_o is the air density, c_o is the air

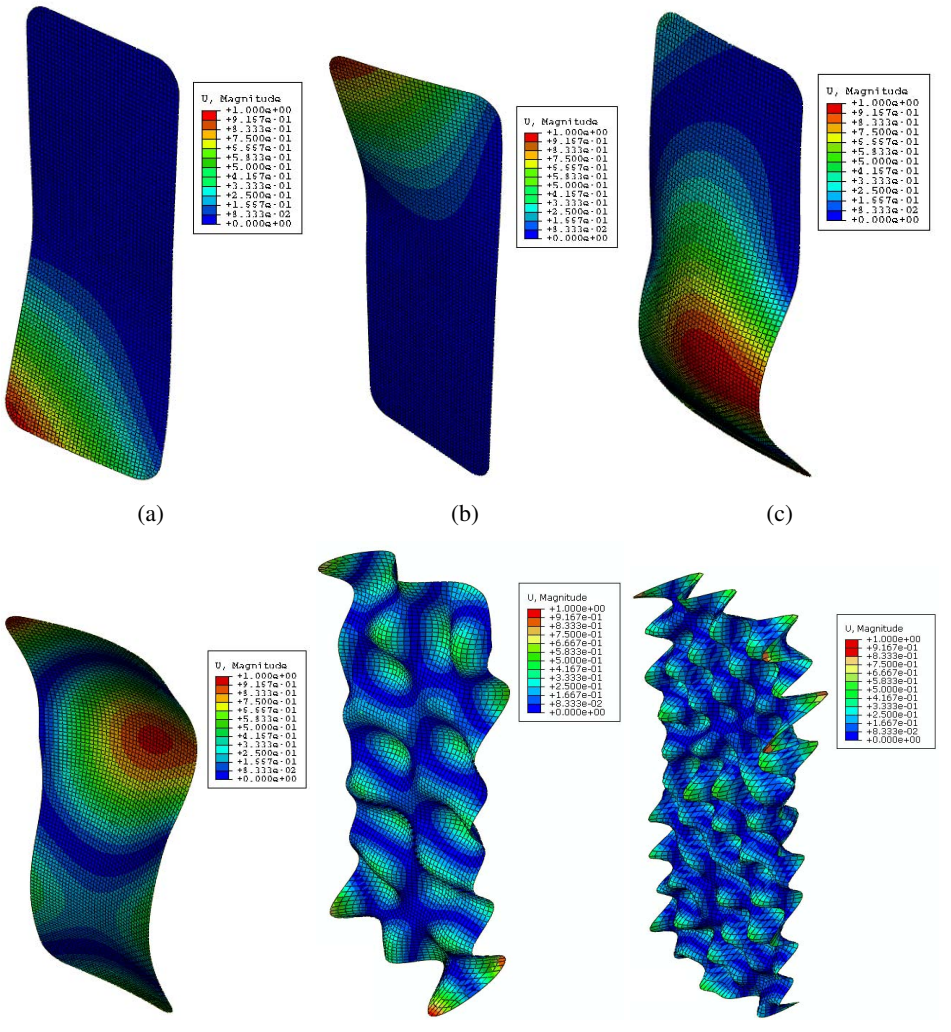

Figure 7: Modal modes and their corresponding natural frequencies. The panel boundary is supported by five-simply-supported points.

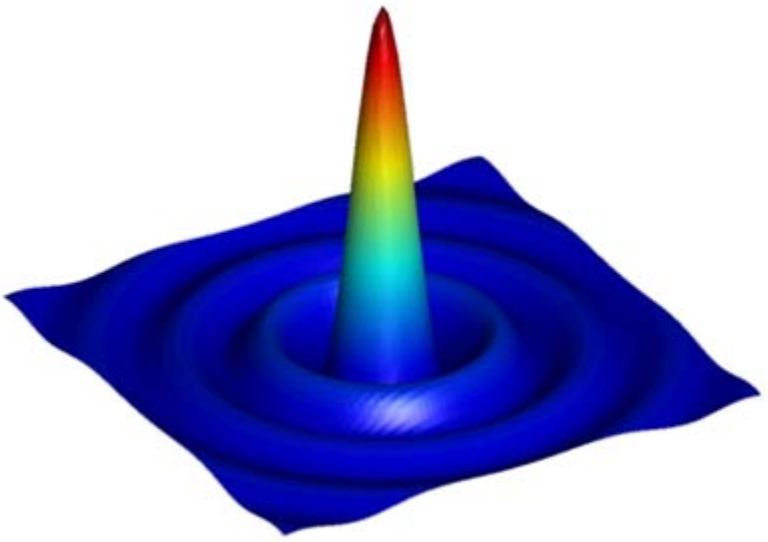

Figure 8: Jinc function

phase speed, k_a is the acoustic wavenumber, k_s is the structural trace wavenumber of the panel, δ is the size of the mesh spacing (= 25 mm on the calculations) and r_{ij} is the distance between two points, i.e. i and j, on the plate. This method computes the total power radiated in the near field, by using the air pressure at every point on the plate due to surface displacements. It is assumed that the total power in the near field is necessarily the same as the total power in the far field.

Fig. 9 shows the panel energy response for a clamped (BC-clamp), simply-supported (BC-SS), 5-point simply-supported and a free (BC-free) boundary panel. It is evident that the energy variation is more significant at lower frequencies. Above 800 Hz, the variation of the panel energy response is within a range of 5 dB approximately. It is seen that the energy variation for the 5-point simply-supported panel is less pronounced than the other three boundary conditions over the whole frequency range considered herein. In other words, the energy distribution over the spectrum seems to be fairly uniform.

Fig. 10 shows the total power radiated (see Eq. 5) by a honey-comb panel for a simply-supported, clamped, free and 5-point simply-supported boundary conditions.

For the 5-point pinned support case (see Table 1), the result shows that the spectrum does not vary as much as for the other boundary conditions. In practical terms,

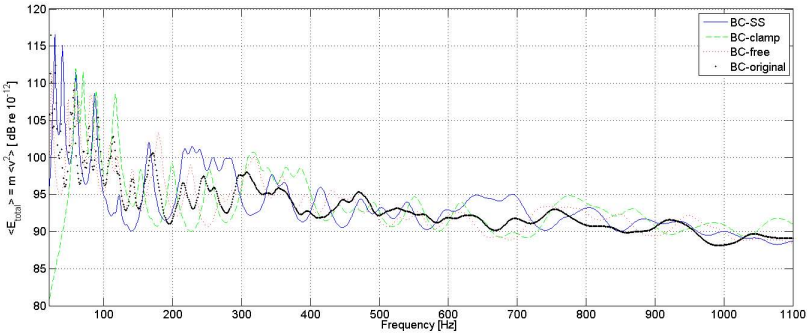

Figure 9: Comparison between panel energy responses for clamped (BC-clamp), simply-supported (BC-SS), 5-point simply-supported and a free (BC-free) boundaries.

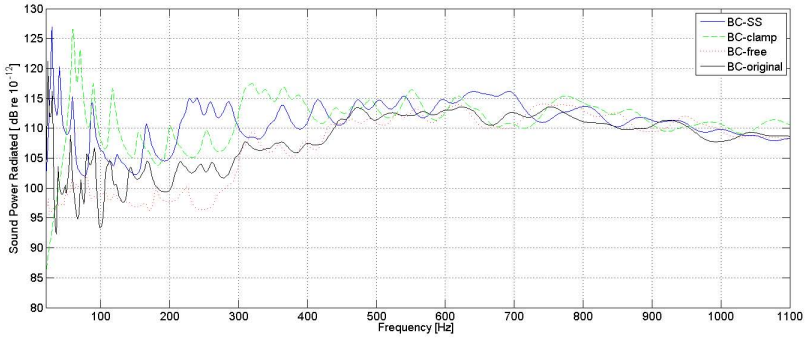

Figure 10: Prediction of the sound power radiated by honey-comb panels using the 'hybrid' method. Four different boundary conditions are considered: clamped (BC-clamp), simply-supported (BC-SS), 5-point simply-supported (BC-original) and a free (BC-free) boundaries.

it might indicate that a more uniform sound power output (and probably a better sound quality) can be achieved using a few simply-support pinned points along the frame.

Fig. 11 shows the simulation for 10 random locations for each one of the 5-point simply-supported positions. The coordinates of each point is shown on Table 2. The variation of the sound power radiated by the honey-comb panel tends to become less pronounced as frequency increases.

Table 1: The Cartesian coordinates of the five-point simply-supported plate (original configuration).

		X(mm)	Y(mm)
	Pos.1	485.0	172
BC-ORIGINAL	Pos.2	485.0	684
	Pos.3	485.0	1115
	Pos.4	0.0	554
	Pos.5	0.0	789

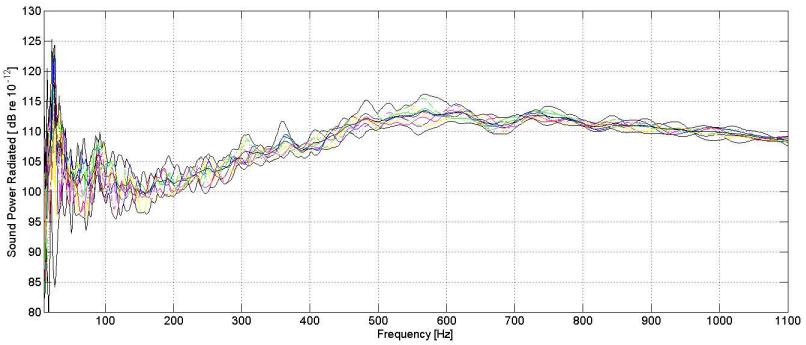

Figure 11: Prediction of the sound power radiated using 10 random locations for the simply-supported points.

Figure 12 shows a comparison made between the most recent computational techniques for sound power radiated from flat panels. It is seen the the Jinc function method is much faster than the FE method when evaluating the total sound power radiation. On the other hand, the SEA method showed to be the fastest one. The main disadvantage of the SEA method is the lack of details and precision at low frequencies.

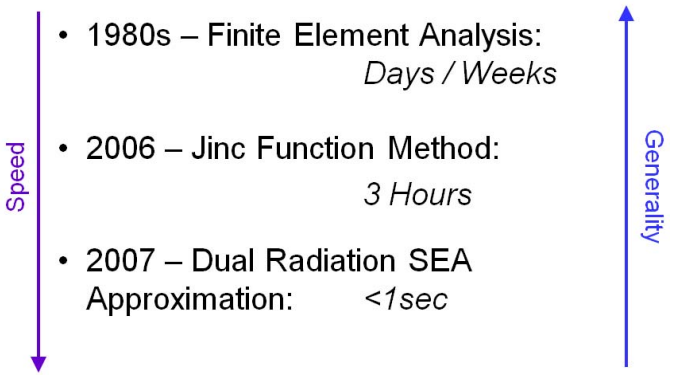

Figure 12: Computational techniques evaluations from the 1980's to 2007.

The radiation efficiency is defined as the ratio of the average acoustic power radiated per unit area of a vibrating surface to the average acoustic power radiated per unit area of a piston that is vibrating with the same average mean square velocity at a frequency for each $ka >> 1$ and the fluid impedances $\rho_o c_o$ should be equal. Thus, it is given by

$$\sigma_{rad} = W_{rad} / \left(\rho_o c_o S < \bar{v}_n^2 >\right) \tag{7}$$

where W_{rad} is total acoustic power radiated and $< \bar{v}_n^2 >$ is the spatial-averaged mean-square normal velocity of the panel.

Figure 13 shows the sound radiation efficiency of the honey-comb panel for different boundary conditions. As expected, the results obtained tend to unit as the dimensionless ratio between the acoustic wavenumber k and the free structural wavenumber k_b also tends to unit. In other words, the sound radiation efficiencies of the panels are not affected by their different boundary conditions at frequencies greater than their critical frequency (f_c =4991 Hz). At very low frequencies, it is seen that the boundary condition for free edge has the lowest radiation efficiency.

4 Conclusions

The purpose of this paper was to investigate the effects of boundary conditions on the sound power radiated from a particular panel. It is seen that for 'irregular' boundary conditions then the hybrid method used herein was appropriate, as the flat panel normal modes were found numerically in advance of applying the Jinc function method. It is believed that this is the first time flat honey-comb type panels have been modeled in this way. Primarily, it seems that the traditional boundary conditions used, (i.e. using simply-supported, clamped or free boundary conditions

Table 2: Coordinates of 11 different boundary condition configurations.

		X (mm)	Y(mm)			X(mm)	Y(mm)
BC-1	Pos.1	485.0	161		Pos.1	485.0	172
	Pos.2	485.0	593	BC-6	Pos.2	485.0	402
	Pos.3	485.0	979		Pos.3	485.0	913
	Pos.4	0.0	763		Pos.4	0.0	280
	Pos.5	0.0	491		Pos.5	0.0	790
		X(mm)	Y(mm)			X(mm)	Y(mm)
	Pos.1	485.0	172		Pos.1	485.0	172
BC-2	Pos.2	485.0	631	BC-7	Pos.2	485.0	402
	Pos.3	485.0	912		Pos.3	485.0	913
	Pos.4	0.0	489		Pos.4	0.0	490
	Pos.5	0.0	841		Pos.5	0.0	790
		X(mm)	Y(mm)			X(mm)	Y(mm)
	Pos.1	485.0	133		Pos.1	485.0	382
BC-3	Pos.2	485.0	631	BC-8	Pos.2	485.0	826
	Pos.3	485.0	1022		Pos.3	485.0	1115
	Pos.4	0.0	590		Pos.4	0.0	709
	Pos.5	0.0	706		Pos.5	0.0	842
		X(mm)	Y(mm)			X(mm)	Y(mm)
	Pos.1	485.0	175		Pos.1	485.0	487
BC-4	Pos.2	485.0	686	BC-9	Pos.2	485.0	1002
	Pos.3	485.0	1015		Pos.3	485.0	1120
	Pos.4	0.0	552		Pos.4	0.0	203
	Pos.5	0.0	788		Pos.5	0.0	354
		X(mm)	Y(mm)			X(mm)	Y(mm)
	Pos.1	485.0	172		Pos.1	485.0	200
BC-5	Pos.2	485.0	402	BC-10	Pos.2	485.0	345
	Pos.3	485.0	631		Pos.3	485.0	1115
	Pos.4	0.0	280		Pos.4	0.0	800
	Pos.5	0.0	790		Pos.5	0.0	1100

for the flat panel which rest on the frame) have provided reasonable uniform results, and in particular at higher frequencies. Nevertheless, the results have shown poor performance over the low frequency range considered, especially at frequencies below 200 Hz, where significant variations occur (+/- 5dB).

A less pronounced variation can be observed when considering the 5-point pinned

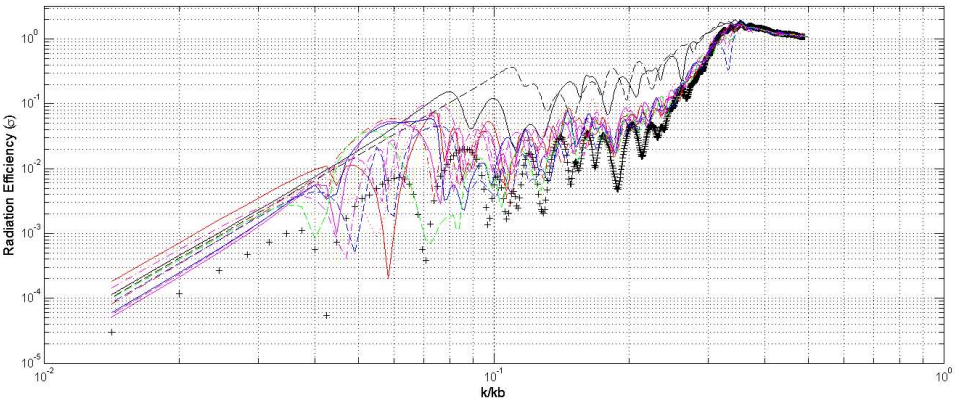

Figure 13: Sound radiation efficiency of honey-comb panels with dimensions equal to 485mm x 1220mm x 5mm and different boundary conditions on the edges. ___ simply-supported boundary; —- clamped boundary; +++ free boundary; color lines for 5-point simply-support randomly positioned (BC_1 - BC_{10} see Table (2))

supported plate at lower frequencies (+/- 3 dB). It is seen that the acoustic response in terms of sound radiation is mainly affected by the boundary condition at low frequencies, as expected. This behaviour indicates the importance of considering the boundary condition effects on sound radiated from honey-comb panels, especially when more complex systems are to be analyzed. The number of modes, and hence the order of the equations, increases significantly and for practical computational and numerical reasons this approach is primarily useful for low frequency predictions. This data might be useful for optimizing sound radiated from this type of panels at low frequencies, where the modal behaviour strongly influences the structure-fluid interaction and consequently the overall sound radiation. Although this research presents the results for a particular panel with simple geometry and material properties, in principle the same procedure can be applied to any other panels with complex features when the mode shapes can be obtained from numerical techniques, such as the FEM/BEM.

As future work, others parameter can be included on the optimization process, such as the panel damping, stiffness and dimensions. The possibility of using non-uniform plates and varying the drive point position might be another area of investigation. In addition, it will also be very useful to compute the sound radiation pattern using for instance the Rayleigh Integral. Furthermore, auralization of radiated signal might be used as a framework to investigate for instance structural failure of a particular panel at some point in space.

In summary, as can be seen above, there are significant opportunities for further development and implementation of the models derived in this study and the author will attempt to continue the investigation. The extension of the 'hybrid' approach to *unbaffled* panels is currently being evaluated.

Acknowledgement: Thanks also to CAPES (Brazilian Research Division of the Ministry of Education), the official sponsor, and to UFMG (Federal University of Minas Gerais – Brazil).

References

Bouayed, K.; Hamdi, M.A. (2012): Finite Element Analysis of the Dynamic Behaviour of a Laminated Windscreen with Frequency Dependent Viscoelastic Core, *J. Acoust. Soc. Am.*, 132(1), pp. 757-766.

Cherrier O.; Pommier-Budinger, V.; Simon, F (2012): Panel of resonators with variable resonance frequency for noise control, *Applied Acoustics*, 73, pp. 781-790.

Cremer, L; Heckl, M.; Petersson, B. A. T. (2005): Structure Borne Sound, *Springer-Verlag Berlin*.

Davy J.L. (2009): The forced radiation efficiency of finite size flat panels that are excited by incident sound. *J Acoust Soc Am*, 126(2), pp. 694-702.

Elliott, S. (2001): The Radiation Efficiency Grouping of Free-Space Acoustic Radiation Modes, *J. Acoust. Soc. Am.*, 109(1), pp. 203-215.

Fahy, F. J. (1985): Sound and Structural Vibration. *Academic Press London*.

Hill, S.G.; Tanaka, N.; Iwamoto, H. (2009): Orthogonal contributor number for the measurement of sound power, *Applied Acoustics*, 70, pp. 1226-1234.

Huang W. C; Chung-fai. N (1998): Sound Insulation Improvement Using Honey-Comb Sandwich Panels, *J. Applied Acoustics*, 53, pp. 163-167.

J. Yan, T.Y. Li, J.X. Liu, X. Zhu (2006): Space harmonic analysis of sound radiation from a submerged periodic ring-stiffened cylindrical shell. *Applied Acoustics*, 67, pp. 743–755.

Langley, R. S. (2007): Numerical Evaluation of the Acoustic Radiation From Planar Structures With General Baffle Conditions Using Wavelets, *J. Acoust. Soc. Am.*, 121, pp. 766-777.

Leppington, F. G.; Broadbent, E.G.; Heron, K.H. (1982): The Acoustic Radiation Efficiency of Rectangular Panel. *CMES: Proceedings of the Royal Society of London. Series A, Math. and Physical Sciences*, 382, pp. 245-271.

Magalhaes, M. D. C; Ferguson, N. S. (2005): The development of a Component Mode Synthesis (CMS) model for three dimensional fluid-structure interaction, *J.*

Acoust. Soc. Am., 118, pp. 3679-3691.

McIntyre, M. E.; Woodhouse, J. (1988): On Measuring the Elastic and Damping Constants of Orthotropic Sheet Materials, *Acta Metall.*, 36, pp. 1397-1416.

Pan, J.; Guo, J.; Ayres, C. (2005): Improvement of Sound Absorption of Honey-Comb Panels, *Proceedings of Acoustics*. Busselton, Western Australia, pp. 195-200.

Pierce, A. D. (1981): Acoustics: An Introduction to its Physical Principles and Applications. *McGraw-Hill New York.*

Putra, A.; Thompson, D.J. (2010): Sound Radiation from Perforated Plates, *Journal of Sound and Vibration*, 329(20), pp. 4227-4250.

Renji, K.; Nair P.S.; Narayanan S. (2001): Non-resonant response using statistical energy analysis. *J Sound Vib.*, 241(2), pp. 253-270.

Xuefeng, Z.; Li, W. (2010): A Unified Approach for Predicting Sound Radiation from Baffled Rectangular Plates with Arbitrary Boundary Conditions, *Journal of Sound and Vibration*, 329(25), pp. 5307-5320.